12345

Vegetation Canopy Anisotropy at 1.4 GHz

Brian K. Hornbuckle, *Member, IEEE,* Anthony W. England, *Fellow, IEEE,*
Roger D. De Roo, *Member, IEEE,* Mark A. Fischman, *Member, IEEE,* and David L. Boprie

Abstract— We investigate anisotropy in 1.4 GHz brightness induced by a field corn vegetation canopy. We find that both polarizations of brightness are isotropic in azimuth during most of the growing season. When the canopy is senescent, the brightness is a strong function of row direction. An isotropic zero–order radiative transfer model could not reproduce the observed change in brightness with incidence angle. Significant scatter darkening was found. The consequence of unanticipated scatter darkening would be a wet bias in soil moisture retrievals through a combination of underestimation of soil brightness (at H–pol) and underestimation of vegetation biomass (at V–pol). A new zero–order model was formulated by allowing the volume scattering coefficient to be a function of incidence angle and polarization. The small magnitude of the scattering coefficients allows the zero–order model to retain its limited physical significance.

Index Terms— Microwave radiometry, vegetation, anisotropy, volume scattering, soil moisture.

I. INTRODUCTION

AT MICROWAVE FREQUENCIES the brightness of a vegetated surface is determined by both the state of the canopy and the underlying soil. The vegetation type, stage of growth, density, temperature, and moisture content, as well as the soil type, roughness, temperature, and moisture content are all important factors. When the canopy has a sufficiently low column density, microwave brightness is most sensitive to the water content of the first few centimeters of the soil [1–3]. At higher column densities, vegetation temperature and moisture content dominate [4]. As the wavelength increases, the microwave brightness originating from the soil suffers less attenuation by vegetation, and the impact of surface roughness and soil and canopy heterogeneity is reduced. Brightness near 1.4 GHz has been identified as the optimum frequency for soil moisture remote sensing.

Recent technological developments [5], [6] have made it feasible to develop satellite 1.4 GHz radiometers that could measure brightness at temporal and spatial scales useful in hydrometeorology [7]. Parallel advances in modeling have produced coupled soil–vegetation–atmosphere transfer (SVAT)

and microwave brightness models which link the remotely–sensed signal to fluxes of energy and moisture between the land and the atmosphere [8–10]. Such work will result in increased understanding of land–atmosphere energy and moisture exchange. This knowledge will, for example, improve our overall grasp of the entire hydrologic cycle [11] and aid in determining whether changes in precipitation [12] and stream flow [13] observed over the past century are part of the natural variability of the system or an indication of a changing climate.

Critical to this vision is the existence of reliable models of land surface microwave brightness. The zero–order radiative transfer model continues to be the model of choice because of its long history of use [14–19] and simplicity. The majority of model validation at 1.4 GHz has occurred near nadir where it has been possible to ignore brightness anisotropy induced by the vegetation canopy.

Through analysis of 1.4 GHz brightness and micrometeorological observations collected in a field of corn, we investigate:

- brightness anisotropy, both in azimuth and elevation; and
- the contribution of volume scattering.

Because of its row structure, we hypothesize that the 1.4 GHz brightness of field corn is anisotropic in azimuth. We also hypothesize that vertically–polarized (V–pol) brightness is anisotropic in elevation while horizontally–polarized (H–pol) brightness is nearly isotropic because of field corn's electrically large vertical stems. Finally, we expect the significance of volume scattering to be higher at V–pol than at H–pol. After testing these hypotheses, we develop a new zero–order model that reproduces the observed phenomena.

II. MEASUREMENTS

Five Radiobrightness and Energy Balance EXperiments (REBEX) were conducted during the spring, summer, and fall of 2001. See Table I for a description of each REBEX and our labeling convention. The experimental site, an 800 m (E–W) by 400 m (N–S) corn field in southeastern Michigan, was unusually flat and uniform in terms of soil properties and vegetation (Figure 1). The soil at the site was a silty clay loam of the Lenawee series (16.1% sand, 55.0% silt, 28.9% clay). Average row spacing was 0.77 m. Plant density was 7.49 m^{-2}. Rows were planted E–W. The field was planted on April 29 and 30 (day of year 119 and 120) and harvested on October 17 and 18 (day of year 290 and 291). Between REBEX–8 and REBEX–8x1, all equipment was removed from the field to accommodate cultivation on June 11 and 12 (day of year 162 and 163). The experiments after cultivation are collectively referred to as REBEX–8x. After June 25 (day of year 176) the fraction of vegetation cover was unity.

Two radiometers, oriented to record H–pol and V–pol 1.4 GHz brightness, were mounted on the hydraulic arm of

B. Hornbuckle and A. England are with the Dept. of Atmospheric, Oceanic, and Space Sciences, and the Dept. of Electrical Engineering and Computer Science, the University of Michigan, Ann Arbor, 48109 USA (e–mail: buckle@umich.edu, england@umich.edu).

R. De Roo is with the Dept. of Atmospheric, Oceanic, and Space Sciences, the University of Michigan, Ann Arbor, 48109–2143 USA (e–mail: deroo@umich.edu).

M. Fischman was formerly with the Dept. of Electrical Engineering and Computer Science at the University of Michigan, and is now at the Jet Propulsion Laboratory, California Institute of Technology, Pasadena, 91109–8099 USA (e–mail: Mark.A.Fischman@jpl.nasa.gov)

D. Boprie is with the Space Physics Research Laboratory, the University of Michigan, Ann Arbor, 48109–2143 USA (e–mail: boprie@umich.edu).

TABLE I

REBEX INFORMATION. DATE INFORMATION INCLUDES DAYS OF YEAR. *GS* REFERS TO VEGETATION GROWTH STAGE. *H* IS VEGETATION HEIGHT IN METERS. *M* IS VEGETATION COLUMN DENSITY IN KG M^{-2}. M_w IS WATER COLUMN DENSITY IN KG M^{-2}. *LAI* IS LEAF AREA INDEX IN M^2 M^{-2}. σ_s IS SOIL SURFACE HEIGHT STANDARD DEVIATION IN MM.

	Dates	*GS*	*H*	*M*	M_w	*LAI*	σ_s
REBEX–8	May 23–25 (143–145)	effectively bare soil	0.2	0.3	0.3	0.1	–
REBEX–8x1	July 4 (185)	growing	1.8	4.8	4.3	3.2	28
REBEX–8x2	July 13 (194)	growing	2.2	5.7	5.0	4.0	28
REBEX–8x3	Aug 17–20 (229–232)	maximum biomass	3.0	8.0	6.3	4.8	25
REBEX–8x4	Oct 10 (283)	senescent	2.8	4.9	2.7	2.5	15

Fig. 1. Truck–mounted radiometers on day of year 178. Antennae oriented at $\theta = 35°, \phi = 60°$. Micro–meteorological station tower can be seen in the background.

a truck. The arm, along with a rotator at the end of the arm, made it possible to change both the incidence angle, θ, and the azimuthal angle, ϕ, of the radiometers. Azimuthal angle was measured with respect to row direction, with $\phi = 0°$ being parallel to the row direction. The truck was positioned within the field at the head of a "lane", a portion of the field that was not planted. The lane, 6 rows wide and approximately 250 m long, began at the eastern edge of the field and continued west. The antenna footprints were located at the head of the lane, to the west ($\phi = 0°$) and to the south ($\phi = 90°$).

Brightness temperatures were measured at incidence angles of $\theta = 15°$, $35°$, and $55°$ shortly after dawn when soil and canopy temperatures were nearly uniform.

Individual brightness temperature measurements of both the antennae and internal reference loads were made at two–minute intervals. The radiometers were calibrated with an absorber and sky. System gain was continually adjusted according to changes in reference load brightness. The NEΔT (standard deviation of brightness temperature) ranged from 0.4 to 0.5 K. During the last experiment, REBEX–8x4, temperature control of the H–pol radiometer was not as tight as during the previous experiments, resulting in an NEΔT of 1.7 K. See Figure 2 for an example of radiometer precision. The accuracy of brightness measurements is estimated to be within ± 2 K. Antennae E– and H–plane half–power beamwidths were approximately $21°$. Side lobe levels were below -20 dB.

A micrometeorological station was located approximately 150 m west of the truck at the approximate center of the field. Near–surface soil moisture and temperature, soil infrared temperature, vegetation infrared temperature, precipitation, wind speed and direction, relative humidity, air temperature, and downwelling solar and atmospheric radiation were recorded on a datalogger system. A vegetation infrared (IR) thermometer was positioned approximately 1 m above the canopy and pointed at nadir. An identical IR thermometer underneath the canopy, approximately 20 cm above the ground and also pointed at nadir, measured the soil surface temperature. These two sensors each have accuracy of $< \pm 0.7$ K and a precision of < 0.1 K. Twenty–minute averages of micrometeorological variables sampled once every ten seconds were recorded. Leaf–area index (LAI) as well as vegetation and water column densities were measured periodically throughout the summer. Each LAI value was computed from the average of ten samples taken at random locations separated by 5 to 10 m within the field. Each sample made using one above–canopy measurement and the average of three below–canopy measurements of the incident radiation: in the row, and one–third and two–thirds of the way across the row space. The wet and dry masses of six randomly chosen plants were averaged to compute column densities. Each plant was separated by component (stem, leaves, and ear).

Several hundred hand-held impedance probe measurements of soil moisture, calibrated with gravimetric samples (150 cm^3 soil scoop) and bulk density measurements (USDA–ARS excavation method), were made over the course of the experiments to calibrate continuous measurements of soil moisture made by buried time-domain reflectometry (TDR) instruments [20].
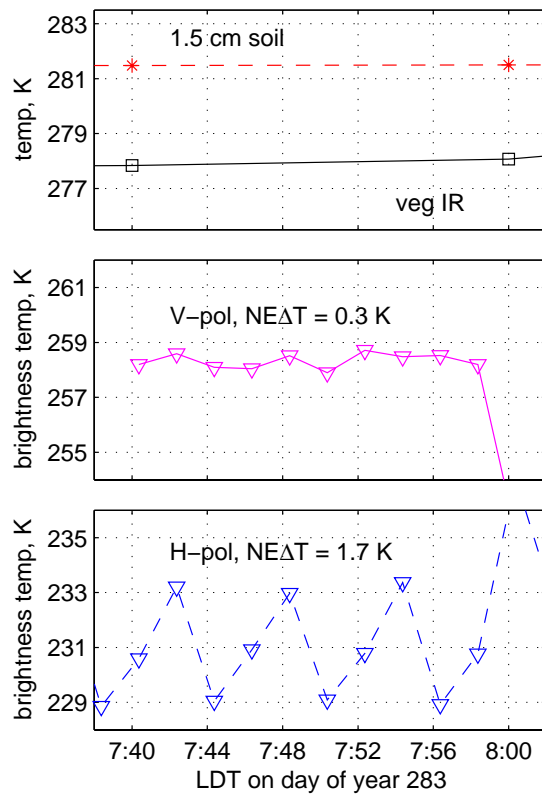
Fig. 2.   An example of radiometer precision during REBEX–8x4. Soil and vegetation temperatures and soil moisture (not shown) were essentially constant during the 20–minute period between 7:40 and 8:00 Local Daylight Time (LDT). Presented NEΔT is for the 10 brightness temperature measurements made during this period.
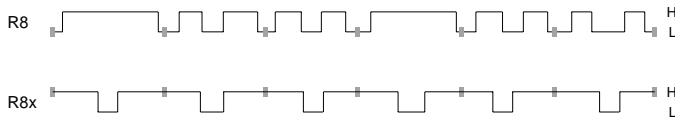
Fig. 3.   Soil topography during REBEX–8 and REBEX–8x reduced to a binary representation.

TDR instruments placed at 1.5 cm and 4.5 cm below the soil surface (which measured the 0–3 and 3–6 cm layers, respectively) matched the 0–6 cm soil water content sampled by the impedance probe. Temperature corrections were applied to all TDR measurements [21]. On days the impedance probe was used, 10 measurements were made in the row and 10 measurements were made between the rows at 7 randomly chosen sites in the experiment area, for a total of 140 measurements per day. This procedure was used to calibrate the TDR instruments in–situ to the *field–average* near–surface soil moisture. As a result of this measurement procedure and the uniformity of the site, the 0–3 and 3–6 cm soil water content data reported in this paper are believed to be accurate to within $\pm 2\%$ by volume with a precision of much less than 1%.

Planting and cultivation produce distinct localized soil topography in agricultural fields. This topography was reduced to a binary representation of high (H) and low (L) areas as a practical way to retain this unique row structure. Figure 3 illustrates the H and L representation. Although only 2 to
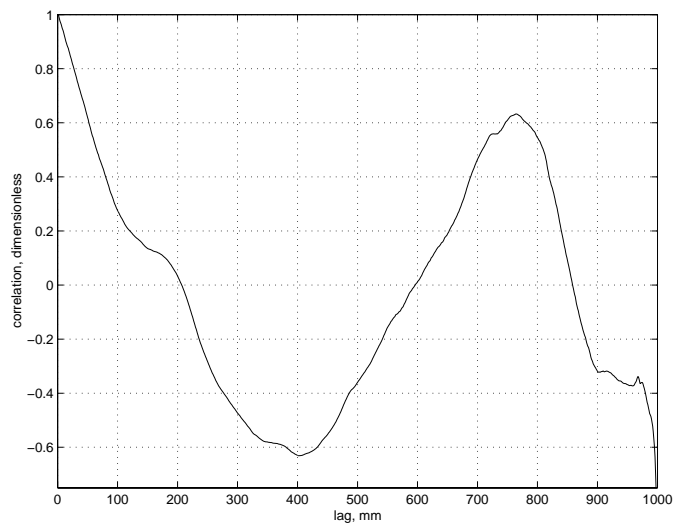
Fig. 4.   Soil surface roughness correlation function, $\rho(l)$, a measure of the height correlation between two points along a transect separated by a lag of l. The correlation length is defined as $\rho(l_c) = 1/e \approx 0.3679$.

4 cm lower than H areas, L areas were distinct from the rest of the soil surface because of their significantly higher water content (and resulting darker color), bulk density, and smoother surface. They tended to be located in the middle of the row space and in the row during REBEX–8, although absent in every third row space. When the soil was cultivated, the top 5 to 7 cm of the soil in the middle of the row space was effectively "pushed" towards the rows, creating a L area in each row space. No distinction was made between trafficked (wheels of tractor or other machinery) and un–trafficked row spaces [22]. The fractions of H and L areas were determined by sampling several rows with a metric tape measure. During REBEX–8, 36% of the soil surface was classified as L. After cultivation, the this fraction changed to 21%. A total of twelve TDR instruments, three in H areas at 1.5 cm, three in H areas at 4.5 cm, three in L areas at 1.5 cm, and three in L areas at 4.5 cm were appropriately averaged together, accounting for the spatial fractions of H and L areas, to produce field–average 0–3 and 0–6 cm water content measurements. The TDR were spread over an approximately 20 m^2 area near the micro–meteorological station tower.

A laser profiler was used to measure soil surface height variations. The profiler had a horizontal resolution of 1 mm and a vertical precision on the order of 10^{-2} mm. Four one–meter transects perpendicular to row direction of undisturbed soil were measured on August 25, 2000, (day of year 238) in a nearby corn field prepared using the same practices as the REBEX–8 field. These four transects were oriented end–to–end and covered seven rows. Figure 4 is a plot of the average correlation function, ρ. The average surface height standard deviation was calculated to be $\sigma_s = 14$ mm and the average correlation length was $l_c = 85$ mm. Strictly speaking, surface segments totaling $40\sigma_s$ and $200l_c$ must be used to accurately characterize these surface parameters [23]. While this condition was satisfied for σ_s, l_c must be considered an estimate. Despite this fact, these soil roughness measurements

are of high quality. The periodic nature of the row structure is clearly evident in Figure 4: note that ρ peaks again at precisely the average row width of 0.77 m. In the case of a periodic surface, the total roughness can be thought of as a random roughness superimposed on a periodic function. Because the random roughness is uncorrelated to the periodic variation, the difference between the two peaks represents this random roughness.

After it is established by tillage, σ_s decreases exponentially with precipitation over the course of the growing season [24]. As noted earlier, σ_s and l_c were only measured once, the year before REBEX–8x. Using precipitation data from a Michigan Automated Weather Network station 10 km east of the REBEX–8x site, the initial value of σ_s after cultivation in early June of 2000 was found to be 36 mm. This value was assumed to be the same for REBEX–8x. Precipitation data was then used to find best estimates of σ_s for REBEX–8x1, –8x2, –8x3, and –8x4. These values are listed in Table I. The correlation length, l_c, was assumed not to change over time.

III. Row Anisotropy

Although spatially heterogeneous on meter scales due to the variable size of plant constituents such as stems, leaves, and ears, a field corn canopy can be considered quasi–continuous at 1.4 GHz [25] and hence treated as a single dielectric layer. Dielectric anisotropy can result in the polarization of electromagnetic waves. As a result, emitted brightness of anisotropic media can depend upon the propagation direction.

Because of the significant row structure of field corn, anisotropy is expected. The stems and ears, essentially moist dielectric rods with thicknesses a significant fraction of the wavelength, are arranged in uniform rows with row spacings of three to four wavelengths at 1.4 GHz. This arrangement is expected to enhance polarization within the row. For example, the variation of the 1.4 GHz brightness temperature of corn as a function of the orientation of cut stalks stripped of leaves and laid on the ground has been observed [26]. An anisotropic random medium model was used to analyze a subset of the data and was able to reproduce the general trends observed [27]. At H–pol, approximately +12 K and +23 K differences between plants oriented perpendicular ($\phi = 90°$) and parallel ($\phi = 0°$) to the look direction at incidence angles of $\theta = 10°$ and $\theta = 40°$, respectively, were observed. At V–pol, plants oriented parallel to the look direction had higher brightness temperatures. Differences between plants oriented perpendicular and parallel to look direction were approximately -20 K and -14 K at incidence angles of $\theta = 10°$ and $\theta = 30°$, respectively.

In another study at 10 GHz, thin dielectric cylinders (0.27 cm diameter, 20 cm length) were arranged in periodic rows on a reflecting background [28]. No difference in the brightness temperature was observed at $\phi = 0°$ and $\phi = 90°$ for $\theta = 20°$ at both V– and H–pol. At other incidence angles, a difference between $\phi = 0°$ and $\phi = 90°$ *was* observed: a +12 K and +8 K difference at V– and H–pol, respectively, for $\theta = 30°$; a +10 K and +8 K difference for $\theta = 40°$, and a +10 K and +6 K difference for $\theta = 50°$. Although the
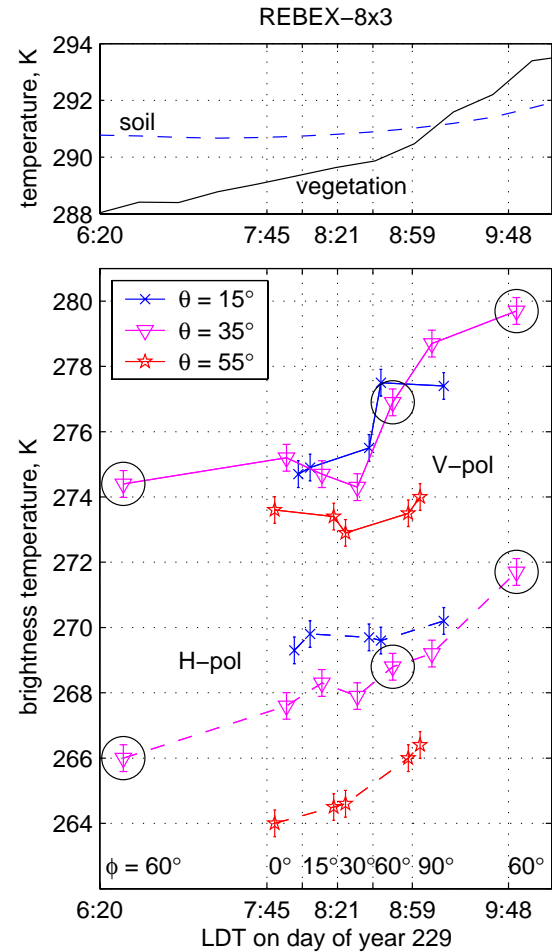
Fig. 5. Time sequence of H–pol and V–pol brightness temperature as a function of angle with respect to row direction (ϕ) during REBEX–8x3. Error bars of $\pm$NEΔT are included. The measurements at $\phi = 60°$ and $\theta = 35°$ are circled. Soil temperature at 1.5 cm and vegetation IR temperature are also plotted.

frequency of observation was 10 GHz, the electrical size of the dielectric cylinders used in this study is similar to the electrical size of stems and ears at 1.4 GHz.

Only one direct measurement of the brightness temperature of a field corn canopy with respect to row direction has been reported [16]. In this study, a +10 K difference between $\phi = 90°$ and $\phi = 0°$ for V–pol brightness temperature at 2.7 GHz was observed for a 5.5 kg m^{-2} vegetation column density corn crop. Row direction experiments were conducted at several points during REBEX–8x. Measurements of H–pol and V–pol brightness at 1.4 GHz collected during REBEX–8x3 for a corn canopy at maximum biomass (vegetation column density of 8.0 kg m^{-2}) at several different angles with respect to row direction and angles of incidence are plotted in Figure 5. These measurements were made during a period of three and a half hours starting at 6:30 LDT (Local Daylight Time) on day of year 229. During the previous night, the radiometers had been left recording data at $\phi = 60°$ and $\theta = 35°$. The last measurements at this position, at 6:32, are the first two points on the left in Figure 5. See Figure 6 for a description of the measurement procedure.

$\phi = 60°$ $\theta = 35°$ 6:32 LDT

CALIBRATION

$\phi = 0°$ $\theta = 55°, 35°, 15°$ 7:45- 8:01

$\phi = 15°$ $\theta = 15°, 35°, 55°$ 8:03- 8:19

$\phi = 30°$ $\theta = 55°, 35°, 15°$ 8:21- 8:37

$\phi = 60°$ $\theta = 15°, 35°, 55°$ 8:39- 8:57

$\phi = 90°$ $\theta = 55°, 35°, 15°$ 8:59- 9:15

CALIBRATION

$\phi = 60°$ $\theta = 35°$ 9:52 LDT
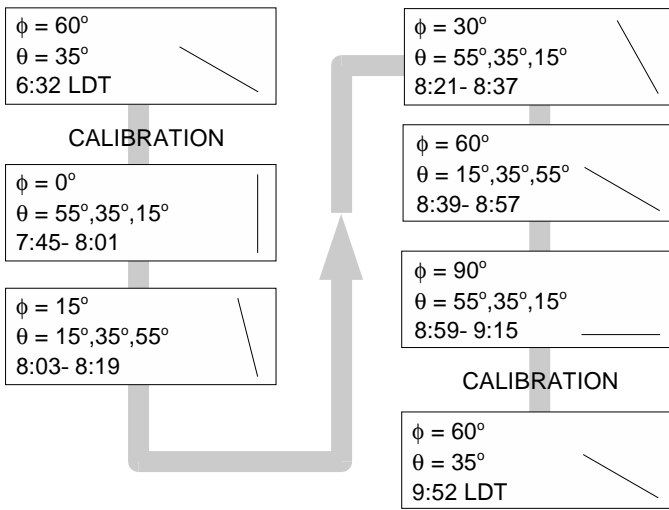
Fig. 6.   Measurement procedure during REBEX–8x3.

TABLE II

RADIOMETER FOOTPRINT SIZE IN TERMS OF THE NUMBER OF ROWS OF CORN THAT WOULD LIE INSIDE OF THE FOOTPRINT. MAXIMUM CANOPY HEIGHT WAS 3.0 M.

	$\phi = 0°$		$\phi = 90°$	
	$z = 0$ m	$z = 3.0$ m	$z = 0$ m	$z = 3.0$ m
$\theta = 15°$	6 rows	4 rows	6 rows	5 rows
$\theta = 35°$	6 rows	4 rows	9 rows	7 rows
$\theta = 55°$	5 rows	3 rows	15 rows	10 rows

Three measurements of brightness temperature, each separated by two minutes, were made at each combination of ϕ and θ in order to verify the measurement precision. Footprint size relative to row spacing is listed in Table II. There was no reason to expect any significant variability in soil moisture among the footprints. The footprint size was always large enough to sample representative fractions of H and L areas.

The general increase in brightness temperatures over the measurement period evident in Figure 5 was due to slowly changing soil and vegetation temperatures. In order to remove this effect, a second–degree polynomial, $T_B(t, \phi = 60°, \theta = 35°, p) = C_1 t^2 + C_2 t + C_3$ (where t is time and p is polarization) was fit to the $\phi = 60°$ and $\theta = 35°$ points circled in Figure 5 at 6:32, 8:49, and 9:52 LDT. These two polynomials were used to approximate the H– and V–pol brightness temperature at $\phi = 60°$ and $\theta = 35°$ at times when the radiometers were measuring the brightness temperature at $\phi \neq 60°$ and $\theta = 35°$. Subtracting these estimated brightness temperatures from the measured data at $\phi = 0, 15, 30,$ and $90°$ and $\theta = 35°$ revealed the variation in microwave brightness as a function of row direction, referenced to the brightness temperature at $\phi = 60°$. In order to remove the temperature change effects from the $\theta = 15°$ and $\theta = 55°$ data, the two polynomials were shifted up to match the recorded data at $\phi = 60°$ and $\theta = 15°$, and shifted down to match the data at $\phi = 60°$ and $\theta = 55°$. In using this compensation procedure derived at $\theta = 35°$ the assumption is made that the weighting of soil and vegetation temperatures does not change with incidence angle. This is not exactly true. At $\theta = 15°$, the soil contribution to the brightness
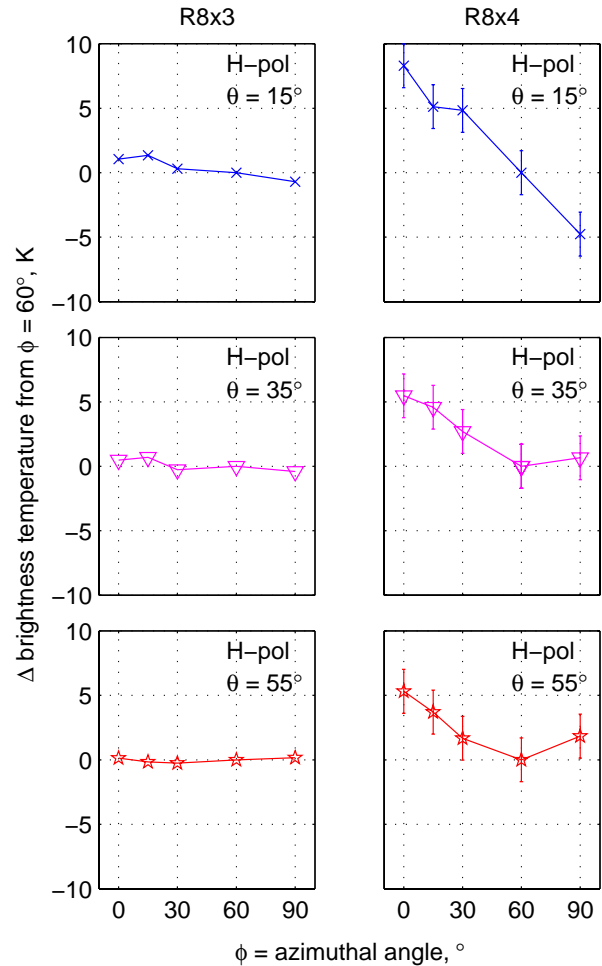
Fig. 7.   Change in H–pol brightness temperature from $\phi = 60°$ as a function of angle with respect to row direction during REBEX–8x3 and –8x4. Error bars on the REBEX–8x4 data are $\pm$NEΔT. The size of the markers on the REBEX–8x3 data are approximately the same size as $\pm$NEΔT and therefore error bars are not included.

temperature is slightly larger than at $\theta = 35°$, while at $\theta = 55°$, the soil contribution is slightly smaller. In either case, the vegetation contribution dominates at higher column densities and the change in relative contribution is small. Figures 7 and 8 present the results.

Contrary to our hypothesis, field corn brightness at 1.4 GHz was *not* a strong function of angle with respect to row direction until senescence. As the corn was growing and when it reached maximum biomass, the observed variation in brightness temperature with ϕ was very small, about 1 to 2 K. Since there were no obvious patterns in these variations, they were probably the result of radiometer precision, the vegetation and soil compensation method, and soil and canopy variability. Despite the absence of a complete set of data for REBEX–8x1 and –8x2, there is no reason to doubt that H–pol brightness temperature is also independent of row direction during this period. When the corn was fully senescent in early October during REBEX–8x4, a consistent pattern did emerge at all incidence angles: H–pol brightness temperatures were highest parallel to the rows at $\phi = 0°$, while V–pol brightness temperatures were highest perpendicular to the rows
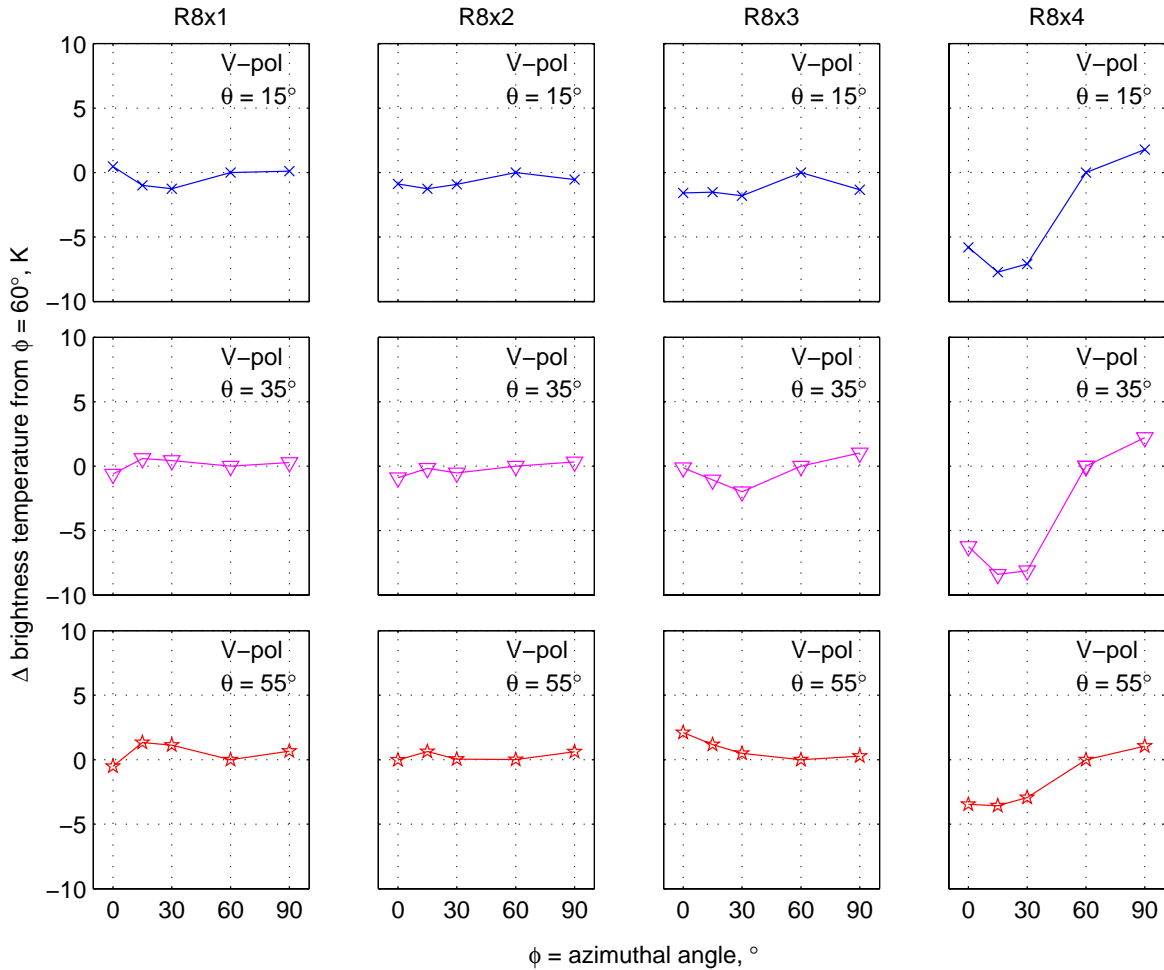
Fig. 8. Change in V–pol brightness temperature from $\phi = 60°$ as a function of angle with respect to row direction during REBEX–8x1, –8x3, –8x3, and –8x4. The size of the markers on the data are approximately the same size as $\pm NE\Delta T$ and therefore error bars are not included.
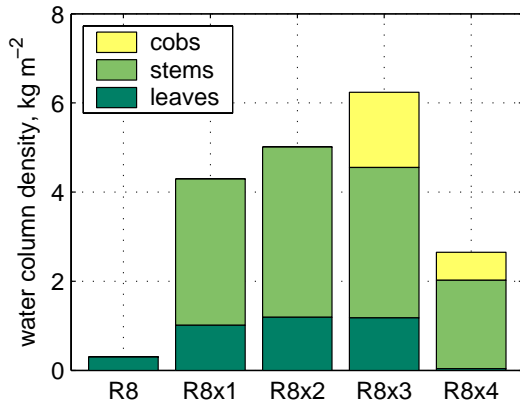
Fig. 9. Distribution of water column density during each REBEX.

at $\phi = 90°$. The V–pol pattern was more complex: although brightness temperatures were lower parallel than perpendicular to the row, the actual minima appeared to be near $\phi = 15°$.

One obvious difference between the synthetic experiments mentioned previously [26], [28] and a real corn canopy is the presence of leaves. At substantially higher frequencies one might in fact expect the brightness temperature to be independent of row direction during the growing season because at shorter wavelengths leaves may "hide" the stems and ears. At 1.4 GHz the leaves are expected to be relatively transparent and hence the internal structure of the canopy should have a significant impact on the brightness temperature. Instead, at 1.4 GHz it appears that leaves either mask the internal, stem–dominated structure within the canopy, or they have a "smoothing" effect. Even the appearance of ears between REBEX–8x2 and REBEX–8x3 did not affect the azimuthal dependence of the brightness temperature. When the canopy dried out after the onset of senescence, the leaves lost their moisture and became essentially invisible at microwave wavelengths. Water column density for each REBEX, separated by plant component, is shown in Figure 9. The stems and ears, which still contained significant moisture, were effectively left "uncovered" once leaf water column density became negligible in REBEX–8x4. This row arrangement of moist stems *was* anisotropic in azimuth, as expected.

IV. ANISOTROPY IN ELEVATION

Because of the natural variation of brightness with incidence angle in isotropic media, a modeling approach, and not simply

an experimental investigation, must be adopted to determine the influence of a field corn canopy on the nature of the emitted microwave brightness in elevation. Within a medium, the incremental change in brightness temperature at each point is the sum of three effects [29]:

$$dT_B(\hat{s}) = -\kappa_e\, T_B(\hat{s})\, ds + \kappa_a\, T\, ds$$
$$+ \frac{\kappa_s}{4\pi} \int_{4\pi} \psi(\hat{s}, \hat{s}')\, T_B(\hat{s}')\, d\Omega'\, ds. \quad (1)$$

First, brightness in the $\hat{s}$ direction is attenuated in proportion to the medium's extinction coefficient, κ_e. Extinction is due to both absorption by the medium (denoted by κ_a, the volume absorption coefficient) and scattering by particles within the medium (denoted by κ_s, the volume scattering coefficient). Second, the medium emits according to its physical temperature, T, in order to maintain thermodynamic equilibrium. Finally, brightness from all other directions $\hat{s}'$ is scattered into the $\hat{s}$ direction according to the normalized phase function $\psi(\hat{s}, \hat{s}')$.

In the simplest case, a vegetated surface can be modeled as a single isothermal layer of vegetation with diffuse boundaries over a soil half space. After applying appropriate boundary conditions, the zero–order solution of (1) can be written

$$T_B = T_{Bsoil} + T_{Bcanopy\uparrow} + T_{Bcanopy\downarrow} \quad (2)$$

where

$$T_{Bsoil} = T_{soil} \times (1 - R_{soil}) \times L \quad (3)$$

$$T_{Bcanopy\uparrow} = (1 - \alpha)(1 - L) T_{canopy} \quad (4)$$

$$T_{Bcanopy\downarrow} = (1 - \alpha)(1 - L) T_{canopy} \times R_{soil} \times L. \quad (5)$$

T_{Bsoil} represents the soil contribution to the total brightness temperature. $T_{Bcanopy\uparrow}$ and $T_{Bcanopy\downarrow}$ represent upwelling and reflected downwelling emission from the vegetation canopy, respectively. T_{soil} is the effective soil temperature; R_{soil}, an effective reflectivity of the soil surface; $L = \exp(-\tau/\cos\theta)$, the transmissivity of the vegetation layer;

$$\tau = (\kappa_a + \kappa_s)\, h = \kappa_e h, \quad (6)$$

the canopy optical depth; h, the canopy height;

$$\alpha = \kappa_s/\kappa_e, \quad (7)$$

the single-scattering albedo; and T_{canopy}, the canopy temperature. Reflected sky brightness, which is only a few kelvin at 1.4 GHz, is neglected. R_{soil} is a function of volumetric water content. τ and α are determined primarily by the structure and water content of the canopy.

The zero–order solution (2) is so named because it neglects radiation scattered into the beam, the mechanism described by the third term of (1). Physically, this approximation is only appropriate in situations of weak scattering where either: $\psi(\hat{s}, \hat{s}') \approx 0$ (little power is scattered into the forward direction); κ_s is small (either the number or the cross section of the scatterers is small); or $\alpha << 1$ ($\kappa_s << \kappa_a$). A non–zero α effectively lowers the vegetation temperature to account for limited volume scattering. Many researchers in the past have used this model for field corn [14], [16]–[19], [30], [31] under the assumption that scattering is small at 1.4 GHz.

TABLE III
CANOPY AND SOIL PROPERTIES DURING BRIGHTNESS TEMPERATURE MEASUREMENTS AT $\phi = 60°$ AND $\theta = 15°$, $35°$, AND $55°$.

	R8	-x1	-x2	-x3	-x4
IR vegetation temp, K	284	292	290	290	278
IR soil surface temp, K	284	293	290	291	278
soil temp @ 1.5 cm, K	285	293	289	291	281
soil temp @ 4.5 cm, K	285	293	291	291	283
vol soil moist 0-3 cm, %	22	13	10	15	25
vol soil moist 3-6 cm, %	25	20	18	19	28

When considering a scattering layer over a homogeneous half–space, scatter–induced change in brightness temperature can be tens of kelvin [32]. Volume scattering is a function of the dielectric contrast between the scatterers in the medium, the dielectric loss of the scatterers, the size of scatterers relative to wavelength, and the fraction of volume filled by the scatterers. If the dielectric constant of the half–space is not significantly larger than the dielectric constant of the scattering layer (as in the case of a vegetation layer over a moist soil half–space) the presence of scatterers reduces the brightness temperature. This phenomena is called *scatter darkening*. For example, scatter darkening has been observed in prairie grass. 19 GHz brightness was correctly predicted with a purely absorptive volume emission model, but model predictions of 37 GHz brightness were too high [10].

Most of the experimental validation of the zero–order model has been at incidence angles close to nadir where the effects of scattering in the canopy are least. One way to test the assumption of weak scattering is to examine the change in brightness temperature with incidence angle. As the impact of the canopy on the microwave brightness increases at progressively larger angles of incidence, can the zero–order solution correctly recreate what is observed experimentally?

Observed 1.4 GHz brightness temperature from each RE-BEX at $\phi = 60°$ and incidence angles of $\theta = 15°$, $35°$, and $55°$ were compared with the predictions of the zero–order model (2). These measurements were made near dawn as part of the row direction experiments. All three incidence angles were measured within a period of less than 20 minutes. Recorded canopy temperatures, soil temperatures, and moisture are listed in Table III. The average of recorded vegetation and soil IR temperatures were used for T_{canopy}. T_{soil} was computed using the parameterization [33]:

$$T_{soil} = T_\infty + (T_{surf} - T_\infty)(\theta_v/w_0)^{B_T} \quad (8)$$

where: T_∞ is a deep soil temperature at 50 cm; T_{surf} is the soil temperature at 1.5 cm; θ_v is the 0–3 cm soil water content; and $w_0 = 0.794$ and $B_T = 0.258$ are empirical parameters. In all cases, T_{soil} and soil temperature measured at 1.5 cm were within 2 K. A dielectric model [34] and measured 0–3 cm soil moisture were used to calculate the specular reflectivity of the soil at the site. The optical depth was computed using a model which relates τ directly to the water column density, M_w, the mass of water in the vegetation per square meter [35]:

$$\tau = bM_w. \quad (9)$$

A value of $b = 0.115$, appropriate for corn at 1.4 GHz when
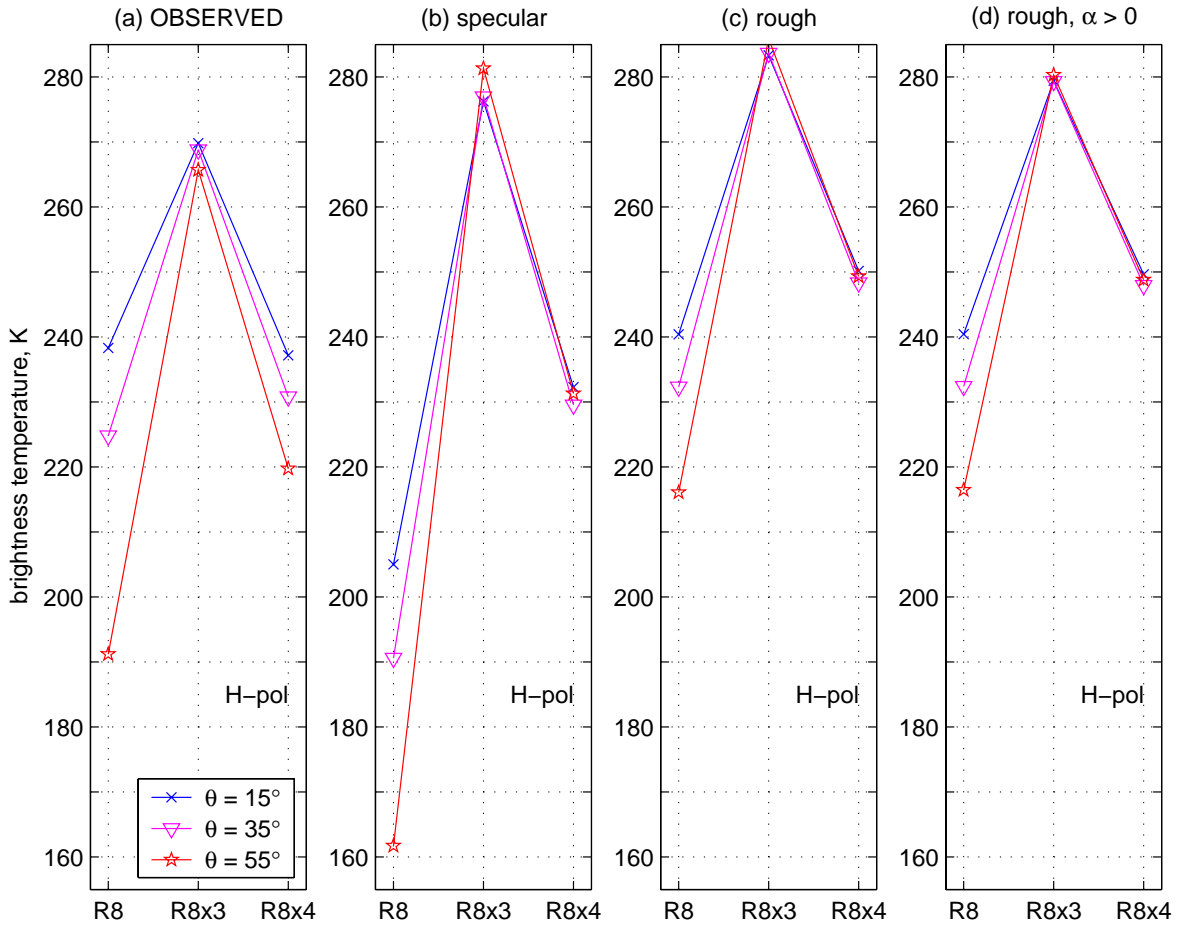
Fig. 10. Observed (a) and modeled (b, c, and d) H–pol brightness temperature during REBEX–8, –8x3, and –8x4. For the model results: (b), the soil surface is specular; (c), the soil surface is rough; and (d), the soil surface is rough and $\alpha > 0$.

$\alpha = 0$, was used [17].

The observations and the model results are compared in Figures 10 and 11. For H–pol, three different versions of the zero–order model were used to illustrate the effect of different physical processes on the brightness temperature. In the first version, part (b) of Figure 10, the soil surface was modeled as specular and α was set to zero. In comparison to part (a), the observed H–pol brightness temperature, it is obvious that the REBEX–8 predictions are too low, but the change in brightness with incidence angle θ is correct. When the amount of vegetation is small, the total brightness temperature is dominated by (3). The measurements and model both followed the Fresnel law: brightness was highest near nadir and decreased as θ increased.

When the canopy reached maximum biomass during REBEX–8x3, the zero–order model no longer correctly predicted the change in H–pol brightness temperature as a function of θ. This is illustrated in part (a) and (b) of Figure 10 by the lines linking the REBEX–8 and –8x3 brightness temperatures. In the model predictions, the lines cross. At large water column densities, canopy emission composes a higher fraction of the total brightness temperature than emission from the soil. As the path length through the canopy increases at larger angles of θ, the zero–order model predicts canopy

emission to increase at a rate which out paces the decrease in soil microwave brightness. The result is that in weakly scattering vegetation canopies, microwave brightness should *increase* with θ when the water column density is large. This is opposite what was observed.

In the second version of the zero–order model, part (c) of Figure 10, the soil was modeled more realistically as rough surface using the model [36]

$$R_{soil,rough} = R_{soil,spec} \times \exp(-h_s) \qquad (10)$$

where: $R_{soil,spec}$ is the specular reflectivity; and h_s is an effective roughness height, computed using the formulation [33]:

$$h_s = A\,\theta_v{}^B (\sigma_s/l_c)^C. \qquad (11)$$

$A = 0.5761$, $B = -0.3475$, and $C = 0.4230$ are empirical parameters, and θ_v is 0–3 cm volumetric soil moisture in units of $m^2\ m^{-2}$. The value of σ_s for REBEX–8x3 was used for REBEX–8 in the absence of a measured value. The REBEX–8 model predictions increased (roughness increases emissivity) and were more in line with the observations of part (a). The remaining differences were likely due to different soil roughness conditions during REBEX–8. Although data used to calibrate (11) was limited to $0° \leq \theta \leq 40°$, a soil surface with significant row structure does not change the variation
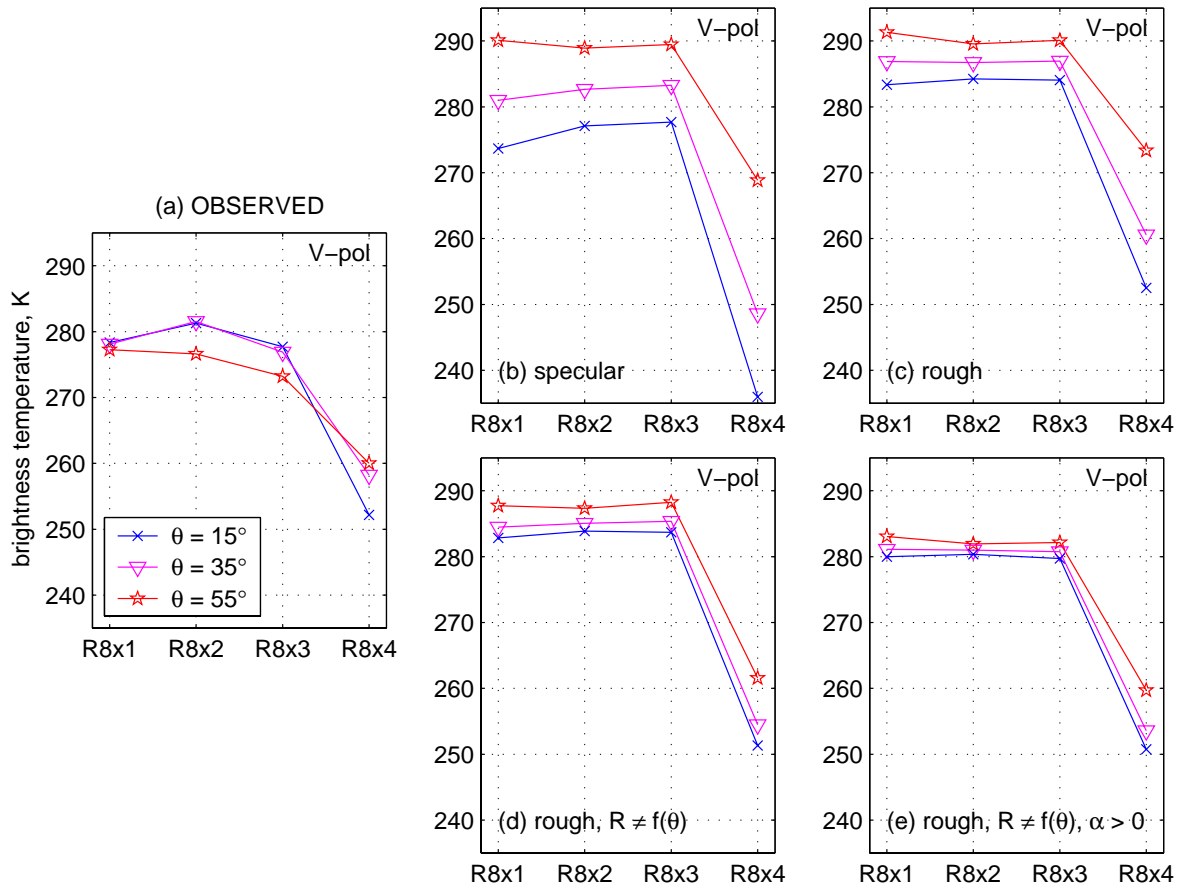
Fig. 11.   Observed (a) and modeled (b, c, d, and e) V–pol brightness temperature during REBEX–8x1, –8x2, –8x3, and –8x4. For the model results: (b), the soil surface is specular; (c), the soil surface is rough; (d), the soil surface is rough and the reflectivity is not a function of θ; and (e), the soil surface is rough, the reflectivity is not a function of θ, and α > 0.

of brightness temperature with incidence angle significantly at H–pol [37]. The REBEX–8x3 relative change is still wrong.

In the the third version of the zero–order model, part (d) of Figure 10, α was set to 0.03 [17] while the modeled soil surface remained rough. This decreased the difference between the three incidence angles for REBEX–8x3, but the modeled change with incidence angle was still opposite that of the observations. For REBEX–8x4, all three versions of the zero–order model predicted a much smaller change in H–pol brightness temperature with incidence angle than what was observed. Evidently, when the canopy is *senescent* it is more *transparent* than predicted by the model. The change with incidence angle is more similar to that of a bare soil surface than that of a vegetation canopy.

Observations at V–pol during REBEX–8x1, –8x2, –8x3, and –8x4 are compared with model predictions in Figure 11. Besides the model versions used to compare H–pol data with observations, a fourth version is used. According to the Fresnel law, V–pol soil microwave brightness increases with θ up to the Brewster angle. The Brewster angle changes with soil moisture and roughness, but it was larger or at least very close to θ = 55° for each data point in part (a) of Figure 11. A soil surface with significant row structure removes much of this effect [37]. As such, in part (d) the strong variation of the soil reflectivity with incidence angle at V–pol was

removed by setting the reflectivity at θ = 15°, 35° and 55° equivalent to the reflectivity at θ = 0°. Although a rough soil surface, removal of the Brewster angle effect, and a non–zero single–scattering albedo all reduced the differences in V–pol brightness temperature between θ = 15°, θ = 35°, and 55°, the observations show that the brightness *decreased* with incidence angle, while the model predicted brightness to *increase* with incidence angle. On the other hand, the model again correctly predicted the relative change with incidence angle for senescent field corn.

In summary, an isotropic zero–order model (2) was not able to reproduce the observed brightness temperature change with incidence angle in field corn. The observed decrease in brightness with θ is likely due to scatter darkening in the canopy since the electrical size of the stems and ears of field corn are significant at 1.4 GHz. This darkening increased with incidence angle. At H–pol, brightness temperatures modeled assuming no scattering were only 1 to 2 K too high at θ = 35° but 7 to 9 K too high at θ = 55° for corn at maximum biomass, assuming that the zero–order model can be fit to observations at θ = 15° by adjusting semi–empirical parameters. For senescent corn, modeled brightness temperatures were even higher, although this was not due to volume scattering but because the canopy is in reality more transparent than predicted by the model: 4 to 5 K too high at θ = 35°, and 16 to 17 K
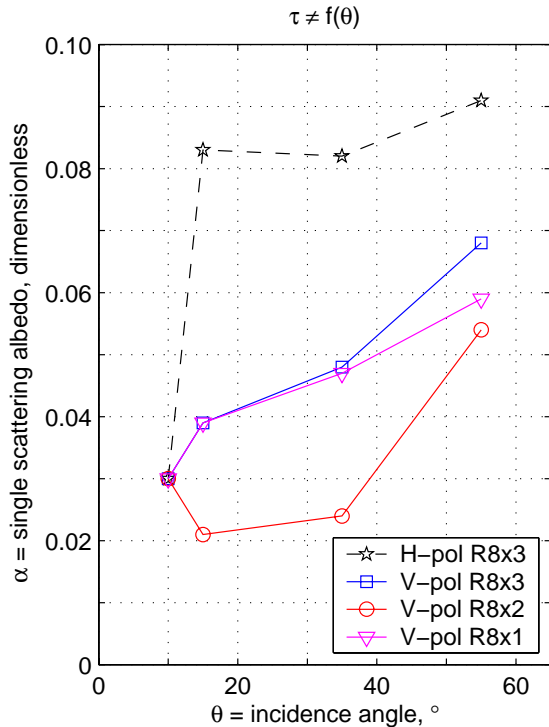
Fig. 12.   Variation of the single scattering albedo, α, with incidence angle, θ. In this method, the optical depth, τ, does not vary with θ.

Fig. 13.   Variation of the single scattering albedo, α, with incidence angle, θ. In this method, the volume absorption coefficient, κ_a, does not vary with θ. As a result, the optical depth, τ, *does* vary with θ.

too high $\theta = 55°$. At V–pol, modeled brightness temperatures were 1 to 8 K too high at $\theta = 35°$ as compared to $\theta = 15°$, and 4 to 18 K too high at $\theta = 55°$ for growing corn and corn at maximum biomass. For senescent corn, modeled V–pol brightness temperatures were 3 K too low to 6 K too high at $\theta = 35°$ as compared to $\theta = 15°$, and 1 to 25 K too high at $\theta = 55°$. Although the zero–order model could not predict the correct change with incidence angle, its predictions steadily improved as the model parameters became more realistic. For the most realistic cases, part (d) in Figure 10 and part (e) in Figure 11, predictions were only at most 2 K too high at $\theta = 35°$ as compared to $\theta = 15°$, and at most 7 K too high at at $\theta = 55°$.

V. NEW ZERO–ORDER MODEL

To accommodate volume scattering, the zero–order model was adjusted to fit the REBEX–8x1, –8x2, and –8x3 data using two methods. Unless otherwise noted, the parameters used in part (d) of Figure 10 and part (e) of Figure 11 were used in this analysis. In the first method, the single–scattering albedo, α, was adjusted to fit the data at each incidence angle, θ. The value of b in (9) was changed to 0.130, appropriate for corn when $\alpha \neq 0$ [17]. In this method the optical depth, τ, does not change with θ. Because α *does* change, it can be seen from (6) and (7) that if α increases with θ, then κ_s increases with θ and κ_a must *decrease* with θ in order to maintain a constant τ. The relationship between α and θ is presented in Figure 12. The points at $\theta = 10°$ are from previous research on field corn brightness [17].

In the second method, both τ and α are allowed to change with θ, but κ_a is held constant. The value of κ_a is determined by the values of τ and α at $\theta = 10°$ [17]. Since $\tau = bM_w = \kappa_e h$, then $\kappa_a = (1-\alpha)\kappa_e = (1-\alpha)(bM_w)/h$. The volume scattering coefficient, κ_s, is then adjusted to match the model to the data. At each new value of κ_s, τ changes in accordance with (6). The relationship between α and θ for this method is shown in Figure 13.

Note that both methods produced nearly identical results. This means that τ can be effectively considered not to be a function of θ. The changes in κ_s, though significant in the final brightness temperature, are small relative to κ_a. The α are, in general, physically–consistent with the assumptions made in formulating the zero–order model. V–pol α increase with θ. The REBEX–8x1 and REBEX–8x3 values match closely. The H–pol α are much higher than previously reported [17], near the limit of $\alpha << 1$. On the other hand, they do not vary much with θ between $\theta = 15°$ and $55°$.

VI. CONCLUSIONS

Both polarizations of the 1.4 GHz brightness of a field corn canopy are isotropic in azimuth during most of the growing season. When the canopy is senescent, brightness is a strong function of row direction. At H–pol, brightness is highest parallel to the rows, while at V–pol, brightness is highest perpendicular to the rows. Brightness temperature changes by 5 to 10 K in azimuth, depending on the incidence angle. Leaves were seen to play an important role: instead of acting simply as a "cloud" of moisture, they scatter microwave radiation at 1.4 GHz and mask the internal, stem–dominated structure of a field corn canopy. At senescence when they lose

their water, they become essentially invisible and the internal structure is exposed. It is also likely that a field corn canopy is essentially isotropic in azimuth at earlier points in the growing season when the leaf column density and fraction of cover are large enough compared to the stem column density. Other row crops that are less heterogeneous (such as wheat, soybeans, and cotton) are likely to have the same qualities.

An isotropic zero–order radiative transfer model, often used because of its simplicity, could not reproduce the observed change in brightness with incidence angle measured in a field corn canopy. Validation of this model by other researchers at 1.4 GHz has occurred only at angles of incidence near nadir. The measurements reported here represent the first reported systematic investigation of the variation with incidence angle. Significant scatter darkening was found as the canopy was growing and when it reached maximum biomass. The variation of scatter darkening with incidence angle was greater at V–pol than at H–pol. When senescent, the canopy appears more transparent at H–pol than predicated by the zero–order model. The zero–order model was able to correctly predict the change in V–pol brightness with incidence angle for a senescent canopy.

A new zero–order model was formulated to account for the observed variation with incidence angle. This was accomplished by allowing the volume scattering coefficient to be a function of incidence angle and polarization. The small magnitude of the scattering coefficients allows the zero–order model to retain its limited physical significance. The values of the single–scattering albedo found at V–pol were in good agreement with previous research. At H–pol, the single–scattering albedo was much higher.

One consequence of these findings is a concern that biophysical processes other than senescence might result in similarly significant changes in brightness. For example changes in the distribution of water among the leaves, stems, and ears within the vegetation canopy, in response to periods of extreme drought or wetness.

The significance of volume scattering in heterogeneous canopies such as field corn is also an important consideration. Although H–pol has traditionally been used to measure soil moisture, future satellite systems will measure brightness temperature at both polarizations and a large variety of incidence angles ($> 60°$) in order to improve ground resolution and to separate soil and vegetation contributions [38]. In this situation the consequence of unanticipated scatter darkening would be a wet bias in soil moisture retrievals, through a combination of an underestimation of soil brightness (at H–pol) and an underestimation of vegetation biomass (at V–pol). Detailed models which fully account for scattering have been recently developed [39], but the zero–order solution is still being used by most researchers in both experimental [19] and modeling studies [40]. It has many advantages: simplicity; a long history of use in many types of vegetation canopies; potentially only a small set of required ancillary data (canopy temperature and water column density), which could be retrieved by another remote sensing methods [41]; and extensive validation. Unfortunately, most of the validation has been done at incidence angles near nadir where the effects

of the canopy, and volume scattering, are small.

Although we observed scatter darkening in a field corn canopy, particularly at large incidence angles, it was not excessive when the most realistic model parameters were used and we have shown that the zero–order radiative transfer solution can correctly model 1.4 GHz brightness (and remain physically consistent) if κ_s is considered to be non–zero and the canopy anisotropic. The inability of an isotropic zero–order model to reproduce observed change in 1.4 GHz brightness with incidence angle will be less drastic in many types of vegetation. Further evaluation of the performance of the zero–order model at large incidence angles in other types of vegetation should be performed to verify this hypothesis.

REFERENCES

[1] T. J. Schmugge, "Remote sensing of surface soil moisture," *J. Appl. Meteor.*, vol. 17, pp. 1549–1557, 1978.

[2] R. W. Newton and J. W. Rouse, Jr., "Microwave radiometer measurements of soil moisture content," *IEEE Trans. Antennas Propagat.*, vol. AP-28, pp. 680–686, 1980.

[3] J. R. Wang, J. C. Shiue, and J. E. McMurtrey, III, "Microwave remote sensing of soil moisture content over bare and vegetated fields," *Geophys. Res. Lett.*, vol. 7, pp. 801–804, 1980.

[4] P. Pampaloni and S. Paloscia, "Microwave emission and plant water content: A comparison between field measurements and theory," *IEEE Trans. Geosci. Remote Sens.*, vol. GE–24, pp. 900–905, 1986.

[5] D. M. Le Vine, "Synthetic aperture radiometer systems," *IEEE Trans. Micro. Theory Tech.*, vol. 47, pp. 2228–2236, 1999.

[6] M. A. Fischman and A. W. England, "Sensitivity of a 1.4 GHz direct–sampling radiometer," *IEEE Trans. Geosci. Remote Sens.*, vol. 37, pp. 2172–2180, 1999.

[7] D. Entekhabi, G. R. Asrar, A. K. Betts, K. J. Beven, R. L. Bras, C. J. Duffy, T. Dunne, R. D. Koster, D. P. Lettenmaier, D. B. McLaughlin, W. J. Shuttleworth, M. T. van Genuchten, M.-Y. Wei, and E. F. Wood, "An agenda for land surface hydrology research and a call for the second international hydrological decade," *Bull. Amer. Meteor. Soc.*, vol. 80, pp. 2043–2058, 1999.

[8] P. J. Camillo, P. E. O'Neill, and R. J. Gurney, "Estimating soil hydraulic parameters using passive microwave data," *IEEE Trans. Geosci. Remote Sens.*, vol. GE–24, pp. 930–936, 1986.

[9] E. J. Burke, R. J. Gurney, L. P. Simmonds, and P. E. O'Neill, "Using a modeling approach to predict soil hydraulic properties from passive microwave measurements," *IEEE Trans. Geosci. Remote Sens.*, vol. 36, pp. 454–462, 1998.

[10] Y.-A. Liou, J. F. Galantowicz, and A. W. England, "A land surface process / radiobrightness model with coupled heat and moisture transport for prairie grassland," *IEEE Trans. Geosci. Remote Sens.*, vol. 37, pp. 1848–1859, 1999.

[11] R. D. Koster, M. J. Suarez, and M. Heiser, "Variance and predictability of precipitation at seasonal–to–interannual timescales," *J. Hydromet.*, vol. 1, pp. 26–46, 2000.

[12] P. Y. Groisman, R. W. Knight, and T. R. Karl, "Heavy precipitation and high streamflow in the contiguous United States: Trends in the twentieth century," *Bull. Amer. Meteor. Soc.*, vol. 82, pp. 219–246, 2001.

[13] E. M. Douglas, R. M. Vogel, and C. N. Kroll, "Trends in floods and low flows in the United States: Impact of spatial correlation," *J. Hydrol.*, vol. 240, pp. 90–105, 2000.

[14] T. J. Jackson, T. J. Schmugge, and J. R. Wang, "Passive microwave remote sensing of soil moisture under vegetation canopies," *Water Resour. Res.*, vol. 18, pp. 1137–1142, 1982.

[15] F. T. Ulaby, M. Razani, and M. C. Dobson, "Effects of vegetation cover on the microwave radiometric sensitivity to soil moisture," *IEEE Trans. Geosci. Remote Sens.*, vol. GE–21, pp. 51–61, 1983.

[16] D. R. Brunfeldt and F. T. Ulaby, "Microwave emission from row crops," *IEEE Trans. Geosci. Remote Sens.*, vol. GE–24, pp. 353–359, 1986.

[17] T. J. Jackson and P. E. O'Neill, "Attenuation of soil and microwave emission by corn and soybeans at 1.4 and 5 GHz," *IEEE Trans. Geosci. Remote Sens.*, vol. 28, pp. 978–980, 1990.

[18] T. J. Jackson, P. E. O'Neill, and C. T. Swift, "Passive microwave observation of diurnal surface soil moisture," *IEEE Trans. Geosci. Remote Sens.*, vol. 35, pp. 1210–1222, 1997.

[19] W. L. Crosson, C. A. Laymon, R. Inguva, and C. Bowman, "Comparison of two microwave radiobrightness models and validation with field measurements," *IEEE Trans. Geosci. Remote Sens.*, vol. 40, pp. 143–152, 2002.

[20] B. K. Hornbuckle, "Radiometric sensitivity to soil moisture relative to vegetation canopy anisotropy, canopy temperature, and canopy water content at 1.4 GHz," Ph.D. dissertation, The University of Michigan, 2003.

[21] M. S. Seyfried and M. D. Murdock, "Response of a new soil water sensor to variable soil, water content, and temperature," *Soil Sci. Soc. Am. J.*, vol. 65, pp. 28–34, 2001.

[22] T. C. Kaspar, S. D. Logsdon, and M. A. Prieksat, "Traffic pattern and tillage system effects on corn root and shoot growth," *Agron. J.*, vol. 87, pp. 1046–1051, 1995.

[23] Y. Oh and Y. C. Kay, "Condition for precise measurement of soil surface roughness," *IEEE Trans. Geosci. Remote Sens.*, vol. 36, pp. 691–695, 1998.

[24] T. M. Zobeck and C. A. Onstad, "Tillage and rainfall effects on random roughness: A review," *Soil & Tillage Research*, vol. 9, pp. 1–20, 1987.

[25] F. T. Ulaby, A. Tavakoli, and T. B. A. Senior, "Microwave propagation constant for a vegetation canopy with vertical stalks," *IEEE Trans. Geosci. Remote Sens.*, vol. GE–25, pp. 714–725, 1987.

[26] P. E. O'Neill, T. J. Jackson, B. J. Blanchard, J. R. Wang, and W. I. Gould, "Effects of corn stalk orientation and water content on passive microwave remote sensing of soil moisture," *Remote Sens. Environ.*, vol. 16, pp. 55–67, 1984.

[27] J. K. Lee and J. A. Kong, "Passive microwave remote sensing of an anisotropic random–medium layer," *IEEE Trans. Geosci. Remote Sens.*, vol. GE–23, pp. 924–932, 1985.

[28] G. Macelloni, P. Pampaloni, S. Paloscia, and R. Ruisi, "Effects of spatial inhomogeneities and microwave emission enhancement in random media: An experimental study," *IEEE Trans. Geosci. Remote Sens.*, vol. 34, pp. 1084–1089, 1996.

[29] F. T. Ulaby, R. K. Moore, and A. K. Fung, *Microwave Remote Sensing: Active and Passive*. Norwood, MA: Artech House, 1981-1986, vol. 1-3.

[30] T. Mo, B. J. Choudhury, T. J. Schmugge, J. R. Wang, and T. J. Jackson, "A model for microwave emission from vegetation–covered fields," *J. Geophys. Res.*, vol. 87, pp. 11 229–11 237, 1982.

[31] P. E. O'Neill, N. S. Chauhan, and T. J. Jackson, "Use of active and passive microwave remote sensing for soil moisture estimation through corn," *Intl. J. Remote Sens.*, vol. 17, pp. 1851–1865, 1996.

[32] A. W. England, "Thermal microwave emission from a scattering layer," *J. Geophys. Res.*, vol. 80, pp. 4484–4496, 1975.

[33] J.-P. Wigneron, L. Laguerre, and Y. H. Kerr, "A simple parameterization of the L–band microwave emission from rough agricultural soils," *IEEE Trans. Geosci. Remote Sens.*, vol. 39, pp. 1697–1707, 2001.

[34] M. C. Dobson, F. T. Ulaby, M. T. Hallikainen, and M. A. El-Rayes, "Microwave dielectric behavior of wet soil – part II: Dielectric mixing models," *IEEE Trans. Geosci. Remote Sens.*, vol. GE–23, pp. 35–46, 1985.

[35] T. J. Schmugge and T. J. Jackson, "A dielectric model of the vegetation effects on the microwave emission from soils," *IEEE Trans. Geosci. Remote Sens.*, vol. 30, pp. 757–760, 1992.

[36] B. J. Choudhury, T. J. Schmugge, A. Chang, and R. W. Newton, "Effect of surface roughness on the microwave emission from soils," *J. Geophys. Res.*, vol. 84, pp. 5699–5706, 1979.

[37] J. R. Wang, R. W. Newton, and J. W. Rouse, Jr., "Passive microwave remote sensing of soil moisture: The effect of tilled row structure," *IEEE Trans. Geosci. Remote Sens.*, vol. GE–18, pp. 296–302, 1980.

[38] Y. H. Kerr, P. Waldteufel, J.-P. Wigneron, J.-M. Martinuzzi, J. Font, and M. Berger, "Soil moisture retrieval from space: The soil moisture and ocean salinity (SMOS) mission," *IEEE Trans. Geosci. Remote Sens.*, vol. 39, pp. 1729–1735, 2001.

[39] M. A. Karam, "A physical model for microwave radiometry of vegetation," *IEEE Trans. Geosci. Remote Sens.*, vol. 35, pp. 1045–1058, 1997.

[40] E. J. Burke, L. A. Bastidas, and W. J. Shuttleworth, "Exploring the potential for multipatch soil–moisture retrievals using multiparameter optimization techniques," *IEEE Trans. Geosci. Remote Sens.*, vol. 40, pp. 1114–1120, 2002.

[41] T. J. Jackson, "Measuring surface soil moisture using passive microwave remote sensing," *Hydrol. Processes*, vol. 7, pp. 139–152, 1993.

Brian K. Hornbuckle received the Sc.B. in Electrical Engineering (Magna Cum Laude with Honors in Engineering) from Brown University, Providence, RI, in 1994, and the M.S.E. in Electrical Engineering (electromagnetics and signal processing) and Ph.D. in Electrical Engineering and Atmospheric, Oceanic, & Space sciences (geoscience and remote sensing) from the University of Michigan, Ann Arbor, in 1997 and 2003, respectively.

From 1994 until 1996 he taught high school chemistry and physics through the Mississippi Teacher Corps program while simultaneously earning an M.A. in Secondary Education (science) from the University of Mississippi, Oxford. While at Michigan he was supported by an NSF Science and Engineering Fellowship and an EPA Science To Achieve Results Fellowship. He is presently a postdoctoral Research Fellow in the University of Michigan Radiation Laboratory.